Structural correlations in Gaussian random wave fields

Isaac Freund and Natalya Shvartsman
Jack and Pearl Resnick Institute of Advanced Technology, Department of Physics, Bar-llan University, Ramat-Gan 52900, Israel
(Received 22 July 1994)

Correlations in the structure of the amplitude, phase, and real and imaginary parts of the wave function of a Gaussian random wave field are derived from both analytical calculations and computer simulations.

PACS number(s): 42.25.Bs, 42.25.Fx, 42.50.Lc, 42.30.Ms

I. INTRODUCTION

It is well known that the amplitude A and phase φ in a random Gaussian wave field (speckle pattern) are statistically independent [1]. This results from the fact that while there are special values for the amplitude—large values at maxima, small ones at minima, etc.—there are no special values for the phase, since any phase value can be turned into any other phase value simply by passing the wave through a uniform phase shifter (glass plate). The amplitude, however, is invariant under such an operation. Accordingly, the phase at any given point is not only uncorrelated with the amplitude at that same point but is also uncorrelated with the amplitude at every other point. Recently, however, we found from experiment [2] that there are significant correlations between the spatial *variations* of the amplitude and the phase at the same point. Here, we examine these correlations theoretically, while correlations between the amplitude and its gradient at one point and the gradient of the phase at another point will be reported on separately. We calculate the joint probability density functions (PDFs) at a given point for various combinations of A, I (intensity), ∇A, ∇I, $\nabla\varphi$, etc., that provide the theoretical basis for our previous empirical findings [2], and we also use these PDFs to uncover structural correlations not discussed previously. In addition, we find here empirically that the maxima, minima, and saddle points of the real or imaginary parts of the wave field tend to be located on a square quasilattice that exhibits significant short-range order. This rather surprising structural relationship is given a partial theoretical basis using a calculation of the autocorrelation function of the field derivatives.

II. AMPLITUDE, INTENSITY, AND PHASE PROBABILITY DENSITIES

Well-known results [1] for the PDF of A and φ that will prove useful later on are $p(A,\varphi)=p(A)p(\varphi)$, $p(\varphi)=1/(2\pi)$, and

$$p(A)=\frac{\pi}{2\langle A\rangle}\left[\frac{A}{\langle A\rangle}\right]\exp\left[-\frac{\pi}{4}\left[\frac{A}{\langle A\rangle}\right]^2\right], \quad (1)$$

where the average amplitude $\langle A\rangle=(\pi\langle I\rangle/4)^{1/2}$ with $\langle I\rangle$ the average intensity in the speckle field, and $\langle A^2\rangle=4\langle A\rangle^2/\pi$. We note that $p(I)$ may be obtained from Eq. (1) by dividing by $2A$ and replacing A^2 with I, and that $\langle I^2\rangle=2\langle I\rangle^2$.

The various other PDFs we require, such as $p(A,\nabla\varphi)$, $p(\nabla A,\nabla\varphi)$, etc., are obtained by using as a starting point an intermediate result contained in a highly useful paper by Ochoa and Goodman [3]. On the way to determining the PDF of ray directions in a Gaussian speckle pattern, these authors give in their Eq. (41) the PDF $p(I,\varphi,I_x,\varphi_x,I_y,\varphi_y)$, where $I_x=\partial I/\partial x$, $\varphi_x=\partial\varphi/\partial x$, etc. Here we restrict ourselves to symmetric source distributions for which the parameters c_x, c_y, and d in this PDF vanish and $b_x=b_y=b$, as this simplifies the ensuing calculations with little practical loss of generality.

We begin by noting that $p(I,\varphi,I_x,\varphi_x,I_y,\varphi_y)$ is independent of φ, which implies that φ is statistically independent of A, I, ∇A, ∇I, $\nabla\varphi$, etc. Integrating $p(I,\varphi,I_x,\varphi_x,I_y,\varphi_y)$ over φ and converting from I and its derivatives to A and its derivatives, we have as our starting point for the calculation of various amplitude-phase correlations

$$p(A,A_x,A_y,\varphi_x,\varphi_y)=\frac{A^3}{4\pi^2\sigma^2b^2}\exp\times\left\{-\frac{1}{2b}\left[\left[\frac{b}{\sigma^2}+\varphi_x^2+\varphi_y^2\right]A^2+A_x^2+A_y^2\right]\right\}, \quad (2)$$

where $2\sigma^2=\langle I\rangle$ and b is related to the second partial derivatives of the field autocorrelation function [Eq. (45) of Ref. [3]]. Defining $\kappa=2\pi/(\lambda Z)$ where λ is the wavelength and Z the distance to the sample, for a uniformly illuminated square of side S, $b=\langle I\rangle(\kappa S)^2/24$, for a uniformly illuminated circle of diameter D, $b=\langle I\rangle(\kappa D)^2/32$, while for circular Gaussian illumination with $1/e$ points separated by W, $b=\langle I\rangle(\kappa W)^2/16$.

The various PDFs may be obtained from Eq. (2) by inserting appropriate delta functions and integrating. As all these calculations follow the same course we provide one illustration and then simply list our final results. $p(\nabla A,\nabla\varphi)$, for example, is obtained from

$$p(\nabla A,\nabla\phi)=\int_0^\infty dA\int_{-\infty}^\infty dA_x\int_{-\infty}^\infty dA_y\int_{-\infty}^\infty d\varphi_x\int_{-\infty}^\infty d\varphi_y\,p(A,A_x,A_y,\varphi_x,\varphi_y)\delta\left[\nabla A-\sqrt{A_x^2+A_y^2}\right]\times\delta\left[\nabla\varphi-\sqrt{\varphi_x^2+\varphi_y^2}\right]. \quad (3)$$

Using the circular symmetry inherent in the combinations $A_x^2+A_y^2$ and $\varphi_x^2+\varphi_y^2$, the integrations are easily carried out in polar coordinate, yielding $p(\nabla A,\nabla\varphi)=p(\nabla A)p(\nabla\varphi)$, and thus a correlation coefficient (defined in Eq. (2.4-11) of Ref. [1]) $\mu(\nabla A,\nabla\varphi)=0$ in accord with our empirical findings [2] based upon previously described computer simulations [4]. $p(\nabla A)$ and $p(\nabla\varphi)$ are given by

$$p(\nabla A)=\frac{\nabla A}{b}\exp\left[-\frac{(\nabla A)^2}{2b}\right], \tag{4}$$

$$p(\nabla\varphi)=\frac{(2\sigma^2/b)\nabla\varphi}{\left[1+\frac{\sigma^2}{b}(\nabla\varphi)^2\right]^2}, \tag{5}$$

$\langle\nabla A\rangle=(\pi b/2)^{1/2}$, $\langle(\nabla A)^2\rangle=2b$, $\langle\nabla\varphi\rangle=\pi b^{1/2}/(2\sigma)$. We also have from Eq. (2), $p(A,\nabla A)=p(A)p(\nabla A)$.

Although A and ∇A are statistically independent, I and ∇I are not since ∇A and ∇I behave qualitatively differently at optical vortices (which correspond to minima of zero intensity) [5–7], and we find

$$p(I,\nabla I)=\frac{\nabla I}{8\sigma^2 bI}\exp\left\{-\left[\frac{I}{2\sigma^2}+\frac{(\nabla I)^2}{8bI}\right]\right\}, \tag{6}$$

$$p(\nabla I)=\frac{\nabla I}{4\sigma^2 b}K_0\left[\frac{\nabla I}{2\sigma\sqrt{b}}\right], \tag{7}$$

where K_0 is the modified Bessel function of order zero [8], $\langle\nabla I\rangle=\pi\sigma(b)^{1/2}$, $\langle(\nabla I)^2\rangle=16\sigma^2 b$, and $\mu(I,\nabla I)=\pi/[2(16-\pi^2)^{1/2}]=0.634$, which is in accord with our computer simulation that yields $\mu(I,\nabla I)=0.637\pm0.008$. This large positive coefficient reflects significant internal structural correlations, and as our computer simulation indicates, is largely due to the fact that at the minima and saddle points of the intensity where $\nabla I=0$, the intensity itself also tends to be small. We note that $p(I,\nabla A)=p(I)p(\nabla A)$, and that $p(A,\nabla I)$ may be obtained from Eq. (6) by multiplying by $2A$ and replacing I with A^2.

The PDF of greatest current interest to us is

$$p(A,\nabla\varphi)=\frac{A^3\nabla\varphi}{\sigma^2 b}\exp\left\{-\frac{A^2}{2\sigma^2}\left[1+\frac{\sigma^2}{b}(\nabla\varphi)^2\right]\right\}. \tag{8}$$

$p(I,V\varphi)$ may be obtained from this result by dividing by $2A$ and replacing A^2 with I. In computing $\mu(A,\nabla\varphi)$ from Eq. (8) we encounter the difficulty that $\langle(\nabla\varphi)^2\rangle$, which appears in the normalization denominator of the correlation coefficient, diverges logarithmically [Eq. (5)]. A useful remedy is the transformation

$$\Phi=\arctan\left[\frac{\pi\nabla\varphi}{2\langle\nabla\varphi\rangle}\right] \tag{9a}$$

which maps Φ onto the interval $0-\pi/2$. The PDF of Φ is then $p(\Phi)=\sin(2\Phi)$, and

TABLE I. Measured (calculated) correlation coefficients $\mu(A^m,\Phi^n)$.

mn	1	2	3	4
1	−0.659 (−0.664)	−0.671 (−0.675)	−0.655 (−0.659)	−0.629 (−0,.632)
2	−0.571 (−0.574)	−0.556 (−0.559)	−0.523 (−0.525)	−0.486 (−0.488)
3	−0.477 (−0.476)	−0.449 (−0.448)	−0.411 (−0.409)	−0.373 (−0.372)
4	−0.393 (−0.385)	−0.360 (−0.352)	−0.322 (−0.315)	−0.287 (−0.281)

$$p(A,\Phi)=\frac{\pi^2\sin\Phi}{4\langle A\rangle}\left[\frac{A/\langle A\rangle}{\cos\Phi}\right]^3\times\exp\left[-\frac{\pi}{4}\left[\frac{A/\langle A\rangle}{\cos\Phi}\right]^2\right], \tag{9b}$$

where we use $\sigma/b^{1/2}=\pi/(2\langle\nabla\varphi\rangle)$ and $\sigma^2=2\langle A\rangle^2/\pi$. Evident from Eq. (9), as well as from scatterplots obtained from our simulation (not shown), are strong correlations of large A with small Φ (and therefore small $\nabla\varphi$) together with strong correlations of small A with large $\nabla\varphi$ ($\Phi\sim\pi/2$). The correlation of large A with small $\nabla\varphi$ reflects a significant association of speckle spots and phase saddles [2], while the correlation of small A and large $\nabla\varphi$ reflects the fact that at optical vortices [5–7] where $\nabla\varphi$ diverges the field amplitude must go to zero in order to keep the wave function single-valued. As expected, $p(I,\nabla\varphi)$ and $p(I,\Phi)$ describe very similar correlations between I and $\nabla\varphi$ or Φ.

A quantitative comparison of Eq. (9) with our computer data may be had by comparing measured and calculated correlation coefficients for moments of the PDF. Using Eqs. (1), (5), and (9) we find $\mu(A,\Phi)=(\pi)^{1/2}(8-3\pi)/\{3[(4-\pi)(\pi^2-8)]^{1/2}\}=-0.664$, in accord with the measured value $\mu(A,\Phi)=-0.659\pm0.007$). In Table I, we compare measurements of $\mu[A^m,\Phi^n]$ with calculation for $1\le m,n\le4$, finding excellent ($\sim1\%$) agreement for all 16 moments.

Although ∇A and $\nabla\varphi$ are statistically independent, ∇I and $\nabla\varphi$ are not, and

$$p(\nabla I,\nabla\varphi)=\left[\frac{1}{8\sigma b^{5/2}}\right]\frac{(\nabla I)^2(\nabla\varphi)}{\left[1+\frac{\sigma^2}{b}(\nabla\varphi)^2\right]^{1/2}}\times K_1\left[\frac{\nabla I}{2\sigma\sqrt{b}}\left[1+\frac{\sigma^2}{b}(\nabla\varphi)^2\right]^{1/2}\right]. \tag{10}$$

Here K_1 is the modified Bessel function of order one [8]. Use of the transformation in Eq. (9a) yields $\mu(\nabla I,\Phi)=(\pi/3)(8-3\pi)/[(16-\pi^2)(\pi^2-8)]^{1/2}=-0.441$, in accord with our computer simulation that gives $\mu(\nabla I,\Phi)=-0.440\pm0.008$. This anticorrelation is due in part to the fact that at an optical vortex $\nabla\varphi$ diverges while ∇I vanishes.

III. REAL AND IMAGINARY STATIONARY POINT CORRELATIONS

As there is no important distinction between the real and imaginary parts of the wave field (a 90° phase shift converts one into the other), it suffices to discuss the real part alone with the understanding that all conclusions apply equally well to the imaginary part. Either or both parts may be measured using heterodyne techniques, so the results obtained here may be verified by experiment as well as by computer simulation.

We denote the real part of the field by $R(x,y)$, its partial derivatives by $R_x = \partial R/\partial x$, $R_y = \partial R/\partial y$, and the zero crossings of R_x (R_y) by Z_x (Z_y). In Figs. 1(a) and 1(b), we display maps of Z_x and Z_y obtained from our computer simulation [4]. As may be noted, the Z_x (Z_y) curves tend to be elongated parallel to the y axis (x axis) and appear to have a well-defined average spacing. This is confirmed in Fig. 1(c), where we plot the normalized autocorrelation function of Z_x from Fig. 1(a). In addition to the peak at the origin, four additional peaks are clearly visible, so that on average there is significant short-range order over much of the wave field. Stationary points (maxima, minima, and saddle points) of R are located at the intersections of Z_x and Z_y, and using an extension of our previous work [9] we have shown that on every zero crossing saddle points *must* alternate with either maxima or minima. An important statistical property of $R(x,y)$ revealed by our computer simulation is that there is a strong tendency for saddles to alternate with maxima on any given zero crossing, while on neighboring (nearly parallel) zero crossings saddles tend to alternate with minima. This, together with the quasiperiodic spacing of the zero crossings, gives rise to a square quasilattice structure whose unit cell contains a saddle point at the cell center and at each cell corner, a maximum at the center of each of a pair of opposite cell sides, and a minimum at each of the centers of the remaining cell sides. This characteristic structure is illustrated in Fig. 1(d), which is based on the zero crossing maps of Figs. 1(a) and 1(b). We note that the average contents of a unit cell—two saddle points, one minimum, and one maximum—are consistent with a long-standing rule due to Longuet-Higgins [10] that equates the total number of saddles in the wave field to the sum of the numbers of maxima and minima minus one.

Neither Fig. 1(c) nor Fig. 1(d) are easily calculated. We can, however, provide a partial theoretical basis for these results by verifying the strong quasioperiodicity of $R_x(x,y)$ using the normalized autocorrelation function

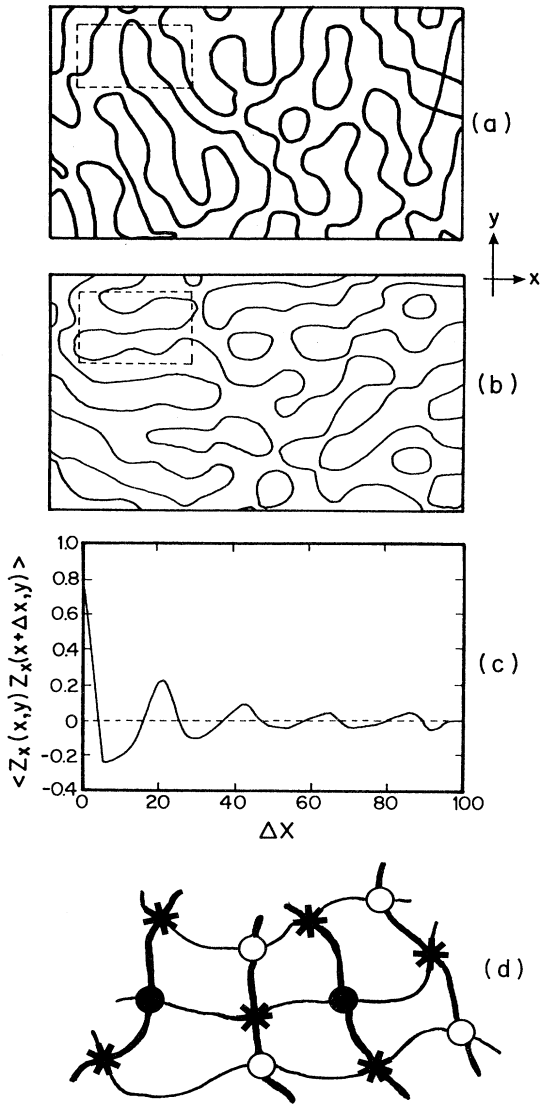

FIG. 1. (a) Zero crossings $Z_x(x,y)$. (b) Zero crossings $Z_y(x,y)$. (c) Autocorrelation function of $Z_x(x,y)$ vs shift Δx in pixels. A coherence length of the field corresponds to 19.2 pixels. (d) Quasilattice fragment formed by the zero crossings contained in the dotted rectangles in the upper left-hand corners of (a) and (b). *, saddle point; ●, maximum; ○, minimum. Most quasilattice fragments tend to be somewhat smaller than this example which contains 1.5 complete unit cells and covers some six coherence areas of the random wave field.

$$\mu_{xx}(\Delta x)=\frac{\langle R_x(x,y)R_x(x+\Delta x,y)\rangle-\langle R_x(x,y)\rangle\langle R_x(x+\Delta x,y)\rangle}{\left\{\left[\left\langle R_x^2(x,y)\right\rangle-\langle R_x(x,y)\rangle^2\right]\left[\left\langle R_x^2(x+\Delta x,y)\right\rangle-\langle R_x(x+\Delta x,y)\rangle^2\right]\right\}^{1/2}}. \tag{11}$$

Other autocorrelations, such as $\mu_{yy}(\Delta x)$, etc., are obtained from Eq. (11) by replacing R_x with R_y, etc. Using the fact that both R and R_x are stationary processes, we have [11] $\langle R_x(x,y)R_x(x+\Delta x,y)\rangle = -\partial^2\langle R(x,y)R(x+\Delta x,y)\rangle/\partial(\Delta x)^2$, and similarly for μ_{yy}. Since the autocorrelation of the real and imaginary parts of the field are identical and the cross correlation between these vanishes, the autocorrelation of the real

part of the field is half the autocorrelation function of the total field. For the circular sample of radius r_s employed in our present computer simulation, the field autocorrelation is given by the Van Cittert–Zernike theorem [1] as $2J_1(u)/u$, where $u=\kappa r_s[(\Delta x)^2+(\Delta y)^2]^{1/2}$ and J_1 is the Bessel function of integer order one [8]. We then obtain

$$\mu_{xx}(\Delta x)=8\left[\frac{J_2(\kappa r_s \Delta x)}{(\kappa r_s \Delta x)^2}-\frac{J_3(\kappa r_s \Delta x)}{\kappa r_s \Delta x}\right], \tag{12a}$$

$$\mu_{yy}(\Delta x)=8J_2(\kappa r_s \Delta x)/(\kappa r_s \Delta x), \tag{12b}$$

and $\mu_{xy}(\Delta x)=\mu_{xy}(\Delta y)=0$. Other autocorrelations such as $\mu_{yy}(\Delta y)$, etc., can be written down by inspection from these results. Measured and calculated autocorrelation functions are compared in Fig. 2, where the excellent agreement between theory and computer experiment is self-evident, as is the strong quasiperiodicity of R_x. Equivalent results hold for R_y, as well as for other sample geometries, so that the structures presented in Fig. 1 represent general properties of Gaussian random wave fields.

IV. SUMMARY

We have found that the spatial variations of the phase and amplitude in a Gaussian random wave field exhibit significant correlations, with large amplitudes being correlated with small phase gradients and vice versa. We also found that large gradients of intensity are correlated with small gradients of the phase, and that there are, in addition, significant correlations of the internal structure of the intensity, with small values of intensity being strongly correlated with small gradients of intensity. The minima, maxima, and saddle points of the real and imaginary parts of the field were found to locally form a face-centered-square quasilattice containing two saddle points, one minimum, and one maximum per unit cell. Our calculations assumed for simplicity a symmetric scattering sample (source). Asymmetric sources can be expected to yield qualitatively similar (although quantitatively different) results that must reduce to the symmetric source results when the asymmetry vanishes. Source asymmetry can also induce new nonzero correlations, such as $\mu_{xy}(\Delta x)$, etc. The structural correlations found here, together with previously discovered near-neighbor correlations between optical vortices [9], demonstrate the existence of substantial hidden order in random Gaussian wave fields. There are undoubtedly many other aspects of this hidden order that remain to be uncovered.

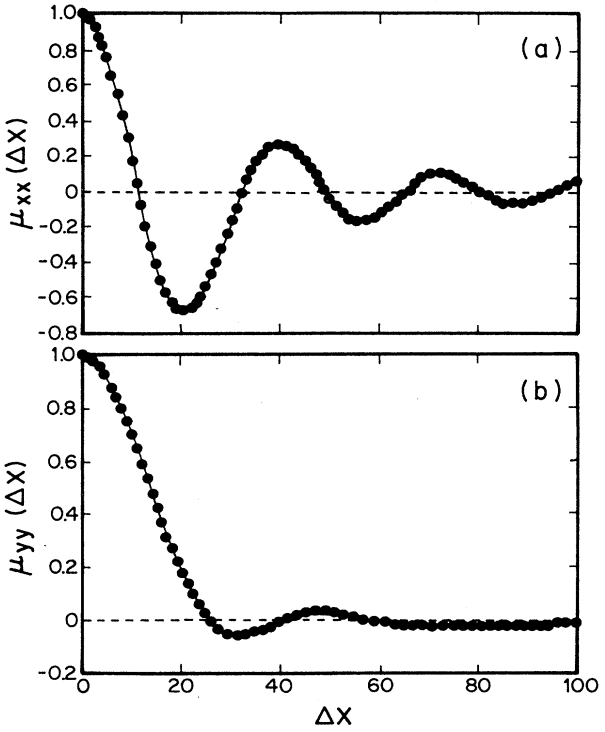

FIG. 2. Autocorrelation functions (a) $\mu_{xx}(\Delta x)$ and (b) $\mu_{yy}(\Delta x)$ vs shift Δx in pixels. As in Fig. 1(c), a coherence length of the field corresponds to 19.2 pixels. ——, calculated [Eq. (12)]; ●, measured. It may be shown from Eq. (12a) that the extrema of μ_{xx} occur at the origin and at the extrema of $J_3(0.2\Delta x)$ (see Ref. [4] for units), so that Δx (extrema)=0, 21, 40, 57, 73, 89, . . ., with first differences of 21, 19, 17, 16, 16, . . ., that illustrate the quasiperiodicity of the autocorrelation.

ACKNOWLEDGMENT

We are pleased to acknowledge the support of the Israel Academy of Sciences and Humanities.

[1] J. W. Goodman, *Statistical Optics* (Wiley, New York, 1985).

[2] N. Shvartsman and I. Freund, Opt. Commun. (to be published).

[3] E. Ochoa and J. W. Goodman, J. Opt. Soc. Am. **73**, 943 (1983). Some related PDFs are given by K. J. Ebeling, Opt. Acta **26**, 1505 (1979).

[4] I. Freund, J. Opt. Soc. Am. A **11**, 1644 (1994). In the present study we use a circular sample of radius $r_s=0.2$ in units where $\kappa=1$.

[5] J. F. Nye and M. V. Berry, Proc. R. Soc. London Ser. A **336**, 165 (1974).

[6] N. B. Baranova, B. Ya. Zel'dovich, A. V. Mamaev, N. Pilipetskii, and V. V. Shkukov, Pis'ma Zh. Eksp. Teor. Fiz. **33**, 206 (1981) [JETP Lett. **33**, 195 (1981)]; N. B. Baranova, A. V. Mamaev, N. Pilipetskii, V. V. Shkunov, and B. Ya. Zel'dovich, J. Opt. Soc. Am. **73**, 525 (1983).

[7] I. Freund, N. Shvartsman, and V. Freilikher, Opt. Commun. **101**, 247 (1993).

[8] *Handbook of Mathematical Functions,* Natl. Bur. Stand. Appl. Math. Ser. No. 55, edited by M. Abramowitz and I. Stegun (U. S. GPO, Washington, DC, 1964).

[9] N. Shvartsman and I. Freund, Phys. Rev. Lett. **72**, 1008 (1994); N. Shvartsman and I. Freund, J. Opt. Soc. Am. A **11**, 2710 (1994); I. Freund and N. Shvartsman, Phys. Rev. A **50**, 5164 (1994).

[10] M. S. Longuet-Higgins, J. Opt. Soc. Am. **50**, 838 (1960).

[11] A. Papoulis, *Probability, Random Variables, and Stochastic Processes* (McGraw-Hill, New York, 1960).